Cancer Science
Japanese Cancer Association JCA
Open Access

Logical design of an anti-cancer agent targeting the plant homeodomain in Pygopus2

Ferdausi Ali,[1] Keiichi Yamaguchi,[1] Mayuko Fukuoka,[1] Abdelazim Elsayed Elhelaly[1] and Kazuo Kuwata[1,2]

[1]United Graduate School of Drug Discovery and Medical Information Sciences, Gifu University, Gifu; [2]Department of Gene and Development, Graduate School of Medicine, Gifu University, Gifu, Japan

Key words

β-catenin, logical drug design, plant homeodomain, Pygopus2, Wnt

Correspondence

Kazuo Kuwata, United Graduate School of Drug Discovery and Medical Information Sciences, Gifu University, 1-1 Yanagido, Gifu 501-1194 Japan.
Tel: +81-58-230-6145; Fax: +81-58-230-6144;
E-mail: kuwata@gifu-u.ac.jp

Funding Information

No sources of funding were declared in this study.

Received April 22, 2016; Revised June 16, 2016; Accepted June 18, 2016

Cancer Sci **107** (2016) 1321–1328

doi: 10.1111/cas.12995

Pygopus2 (Pygo2) is a component of the Wnt signaling pathway, which is required for β-catenin mediated transcription. Plant homeodomain (PHD) finger in Pygo2 intercalates the methylated histone 3 (H3K4me) tail and HD1 domain of BCL9 that binds to β-catenin. Thus, PHD finger may be a potential target for the logical design of an anti-cancer drug. Here, we found that Spiro[2*H*-naphthol[1,2-*b*]pyran-2,4′-piperidine]-1′ethanol,3,4-dihydro-4-hydroxy-α-(6-methyl-1*H*-indol-3-yl)) termed JBC117 interacts with D339, A348, R356, V376 and A378 in PHD corresponding to the binding sites with H3K4me and/or HD1, and has strong anti-cancer effects. For colon (HCT116) and lung (A549) cancer cell lines, IC_{50} values were 2.6 ± 0.16 and 3.3 ± 0.14 μM, respectively, while 33.80 ± 0.15 μM for the normal human fibroblast cells. JBC117 potently antagonized the cellular effects of β-catenin-dependent activity and also inhibited the migration and invasion of cancer cells. *In vivo* studies showed that the survival time of mice was significantly prolonged by the subcutaneous injection of JBC117 (10 mg/kg/day). In conclusion, JBC117 is a novel anti-cancer lead compound targeting the PHD finger of Pygo2 and has a therapeutic effect against colon and lung cancer.

Wnt signaling pathway is important in numerous cellular processes, including differentiation and proliferation of cells, as well as normal embryonic development.[1,2] The key effector protein of this pathway is β-catenin, which is also a potent oncogene.[3] In the absence of Wnt ligands, β-catenin binds to APC, GSK3β and Axin to form a cytoplasmic destruction complex that phosphorylates serine residues in β-catenin, causing proteasomal degradation (Fig. S1a).[1] When Wnt binds to the receptor protein frizzled (FZD) and low-density lipoprotein receptor 5/6 (LRP5/LRP6), disheveled (Dvl) is recruited to the receptor complex (Fig. S1b). This sequesters Axin from the degradation complex.[4] Then β-catenin survives the degradation fate and, subsequently, translocates to the nucleus. Nuclear β-catenin directly binds with T Cell Factor 4/Lymphoid Enhancer Factor (TCF4/LEF) and stimulates the transcription of Wnt genes (Fig. S1b).[5] Dysregulation of the Wnt signaling pathway is implicated in various human cancer types, including colon and lung cancers.[3,5] In general, mutations in genes encoding central components of the Wnt signaling pathway and destruction complex lead to nuclear β-catenin accumulation and contribute to tumor initiation and progression.[3,5,6]

Pygopus2 (Pygo2) is a recently discovered Wnt signaling component that is essential for β-catenin-mediated transcription during normal development.[7–10] Pygo2 recognizes modified histone 3 (H3K4me) tails[6] by their cysteine-rich zinc-binding PHD domain and the HD1 domain of BCL9, an adaptor protein that directly binds to β-catenin (Fig. S1b inset).[8,9,11] Thus, PHD is critical for β-catenin-dependent transcriptional switches in both normal and malignant tissues.[6,12,13] Because the PHD domain is pivotal for Pygo2 function, the interfaces with its binding partners (Fig. S1b inset, red) may represent promising targets for inhibiting the oncogenic function of β-catenin.[7,14] Recently, Pygo2 overexpression has been reported in ovarian,[15] breast,[16] cervical,[17] hepatic[18] and lung cancers.[19]

Lung cancer is the most frequently diagnosed cancer in men in developed countries. In 2012, approximately 1.8 million new lung cancer cases were diagnosed, which accounted for 13% of total cancers.[20] Colon cancer is the third most common newly diagnosed cancer and the third most common cause of cancer death among US men and women. According to the American Cancer Society, approximately 136 830 people were diagnosed with colon cancer in 2014.[21] Current treatment strategies for both lung and colon cancers include surgical resection, chemotherapy, targeted therapy or a combination of these. Recently, small molecules were developed as therapeutic agents to treat lung and/or colon cancer, but few of them were effective. Because the chemical space of small molecules (M.W. approximately 500) is large (approximately 10^{60}), it is essential to establish a logical way to determine the optimum compound that is useful for the treatment of cancers.

Here, we targeted the PHD finger, which is the histone-binding surface of Pygo2. We performed *in silico* screening using logical drug design (LDD) to identify the chemical chaperones[22] based on the 3-D structure of PHD (PDB ID: 2XB1) complexes with HD1 of BCL9.[6] Recent success in drug discovery using LDD for prion[22] has boosted hope for the application of LDD to anti-cancer drug development. We identified a compound, JBC117, which binds to the histone pocket of the

PHD finger and interferes with its binding to histone tails and also to HD1. Furthermore, we demonstrated that JBC117 is a potential antitumor drug based on its therapeutic effects in HCT116 and A549 cells as well as in nude mice with human colon and lung xenografts.

Materials and Methods

Details of surface plasmon resonance (SPR), protein expression and purification, invasion assay, wound healing assay, soft agar assay, colony formation, toxicity, combination index analysis and tumor histopathology and immunohistochemistry are provided in Data S1.

Virtual screening. To identify a potential anticancer compound, we performed structure-based *in silico* screening using the NAGARA program.[23] The Asinex subset (containing approximately 360 000 compounds) of the LigandBox database was used for ligand screening. Chain C was picked from 2XB1 (PDB code) for docking. The docking area which covers the PHD was selected and the size of the grid box was 36 Å × 35 Å × 33 Å. The parameter settings for Auto Dock Vina included exhaustiveness value 8; maximum number of generated binding modes 20; and maximum difference between energies of the best and the worst binding modes 4 kcal/mol; and other optional settings were set to their default values.

NMR measurement. ^{15}N-uniformly labeled recombinant PHD (327–387) was prepared in 20 mM Tris–HCl buffer containing 100 mM NaCl, 20 μM $ZnCl_2$ and 1 mM DTT dissolved in 98% H_2O/2% D_2O. NMR spectra were measured at 25°C on a Bruker Avance600 spectrometer (Bruker BioSpin, Rheinstetten, Germany). NMR data were processed by TOPSPIN-NMR software and peaks were picked using Sparky. Resonance frequencies were identified using the chemical shift lists on PHD (327–387).[6] For the chemical shift perturbation experiment, 100 μM of uniformly ^{15}N-labelled PHD (327–387) was prepared in 20 mM Tris–HCl buffer supplemented with 5% DMSO and 2% D_2O with or without 500 μM JBC117 in a 5-mm-diameter Shigemi microtube.

Cell culture. The human colon cancer cell line HCT116 and lung cancer cell line A549 were used. The HCT116 cell line was purchased from the American Type Culture Collection (Manassas, VA, USA) and A549 cell line was obtained from the RIKEN cell bank (Tsukuba, Japan). DMEM (GIBCO by Life Technologies, Carlsbad, CA, USA) medium supplemented with 10% FBS (GIBCO), 100 units/mL penicillin (GIBCO) and 100 μg/mL streptomycin (GIBCO) were used for cell culture. Cells were then incubated at 37°C in a humid incubator with 5% CO_2.

Cell proliferation and Caspase 3/7 activity assay. Cell proliferation assay (Cell Counting Kit-8; Dojindo, Kumamoto, Japan) and Caspase 3/7 activity (Promega, Madison, WI, USA) were performed according to the manufacturer's instructions.

Transfection and luciferase assay. HCT116, SW480 and A549 cells were cultured on 96-well plates with 1×10^4 cells/well in DMEM with 10% FBS. After ≥70% confluence was reached, each well was transfected with 50 ng TOPFLASH or FOPFLASH (EMD Millipore, Billerica, MA, USA) and 5-ng pRL *Renilla* luciferase (Promega) for normalization. The transfection reagent used was Lipfectamine (Invitrogen, California, USA). After 18 h of transfection, the medium was aspirated and cells were added with 75 μL of culture media containing different concentration of JBC117 with 10 mM LiCl. DMSO was used as control. After 24 h, Firefly and *Renilla* luciferase activities were detected with the Promega Dual Luciferase Assay System (Promega) according to the manufacturer's protocol.

RNA extraction and reverse transcription and quantitative PCR. Total RNA was extracted using the RNeasy Mini Kit (Hilden, Germany) according to the manufacturer's instruction. cDNA was synthesized using a Rever Tra AceR q PCR-RT Kit (TOYOBO, Osaka, Japan). Quantitative RT-PCR was performed using SyBR premix Ex Taq (TAKARA, Shiga, Japan). The PCR primers were *GAPDH* (forward: 5′-GGAGCGAGATCCCTCC-3′ and reverse: 5′-GGCTGTTGTCATACTT-3′); *c-myc* (forward: 5′-TGATCTTGAGGCTGTTGTCATA-3′ and reverse: 5′-ATCTTTCAGTCTCAAGACTCAGCCA-3′) *cyclinD1* (forward: 5′-CCTGTCCTACTACCGCCTCA-3′ and reverse: 5′-TCCTCCTCTTCCTCCTCCTC-3′) *Axin2* (forward: 5′-CAAGGGCCAGGTCACCAA-3′ and reverse 5′-CCCCCAACCCATCTTCGT-3′).

Western blot analysis. Cells were treated with the test compound at different concentrations for 72 h. Cell lysates were prepared with RIPA lysis buffer (10 mM Tris–HCl, pH 7, 150 mM NaCl, 5 mM EDTA, 1% Triton-X, 1 mM DTT, 0.1 mM PMSF, 5% glycerol) supplemented with protease inhibitor cocktails (Sigma-Aldrich). The protein concentration was measured by bicinchoninic acid assay. 20 μg protein samples were loaded on the 15% SDS-polyacrylamide gel and electrophoresed. Primary antibodies used were anti c-myc (Sigma-Aldrich, St. Louis, Missouri, U.S), cyclinD1 (MBL, Nagoya, Japan) and anti β-actin (Sigma-Aldrich, St. Louis, Missouri, U.S.). The immunoblots were detected with an enhanced chemiluminescence detection kit (Thermo Scientific) and a LAS 1000 UV mini-analyzer (Fuji Film, Tokyo, Japan). β-actin was used as an internal control.

Xenograft studies in nude mice. Six-week-old female BALB/c nude mice (purchased from Chubu Kagaku Shizai, Nagoya, Japan) were inoculated subcutaneously in the flank area with 1.5×10^7 cancer cells in 100 μL of DMEM medium with 10 mg/mL Matrigel BD Biosciences, New Jersey, U.S. Tumor growth was measured with calipers once every 2 days and was calculated using the following formula: tumor volume (mm^3) = 0.5 (length × height × width). The tumors were allowed to grow to an average volume 225 mm^3 before initiation of the therapy. Mice were treated with 20 mg/kg/day of JBC117 or ICG001. DMSO (5%) and polyethylene glycol (40%) were diluted with 1× PBS buffer and used as a control. At the end of the experiment, mice were killed and tumors were extracted and immediately fixed in 70% ethanol for histopathology. All procedures were approved by the Committee for Animal Research and Welfare of Gifu University.

Results

***In silico* screening for anti-cancer agents targeting the PHD domain of Pygo2.** To screen for potential small molecules that specifically target Pygo2, a compound library containing approximately 360 000 compounds from ASINEX (New York, USA) was used to dock the PHD domain (a.a. 327–387) (PDB ID: 2XB1) using the docking simulation module of NAGARA.[23] The small molecules were selected based on their energy scores, excluding those with the unusual binding mode by the visual inspection. A total of 103 compounds were selected for the initial *ex vivo* screening for anticancer effect.

***Ex vivo* screening of the selected compounds.** Selected compounds were purchased from Asinex (New York, USA) and their anti-cancer efficacy was examined in human colon

(HCT116) and lung cancer (A549) cell lines using the cell proliferation assay (Fig. S2a). Among these, three compounds (JBC077, −078 and −079) significantly suppressed the proliferation of both colon and lung cancer cells. JBC079 showed the highest anti-proliferative activity among them and was considered as the lead compound. We optimized the chemical structure of JBC079 by investigating the efficacy of its 34 derivatives (Fig. S2b). Finally, we found that the JBC117 ($C_{28}H_{30}N_2O_3$, molecular weight 442.5), (Fig. 1a) had the most potent effect against colon and lung cancer.

Therapeutic potential of JBC117. To evaluate the *ex vivo* cellular effects of JBC117, HCT116 and A549 cancer cells were treated with various concentrations of JBC117 for 72 h by cell proliferation assay. JBC117 exhibited anti-proliferative activity in a dose-dependent manner in both cell lines (Fig. 1b). Time-dependent changes are also shown in Figure S3(a). We used ICG001 (a novel small molecule inhibitor of Wnt signaling pathway that selectively bind to CBP and prevents its interaction with β-catenin)[24] as a positive control. JBC117 had an IC_{50} of 2.6 ± 0.16 and 3.3 ± 0.15 μM for HCT116 and A549 cancer cell line, respectively (Fig. 1c). In addition, we found that JBC117 is superior to ICG001 in suppressing the growth of cancer cell lines (Table 1). We determined the toxicity of JBC117 in normal human fibroblast cell 2F0-C75 (Fig. S3b,c). Normal human fibroblast cells were less sensitive to JBC117 (IC_{50} 33.8 ± 0.15 μM) compared with HCT116 or A549 cells. Moreover, cancer cells treated with JBC117 were analyzed for caspase 3/7 activity. As shown in Figure 1(d), colon and lung cancer cells treated with JBC117 showed significant increase in caspase 3/7 activity.

Interaction between PHD finger of Pygo2 and JBC117. ^{1}H-^{15}N heteronuclear single quantum coherence (HSQC) NMR spectra were measured to identify the interaction sites between JBC117 and PHD finger of Pygo2. Figure 2(a) shows the superimposition of HSQC spectra of PHD finger with (red) and without (black) JBC117. As shown in Figure 2(b), five peaks corresponding to D339, A348, R356, V376 and A378 showed chemical shift alterations. Residues with significant perturbations were mapped onto the 3-D structure of PHD (PDB ID: 2XB1) in Figure 2(c). D339 is located at the K4me pocket of the PHD, whereas A348, A378 and V376 are located at the PHD–HD1 interface. These interactions may affect histone binding as well as binding between PHD and HD1.[6]

The dissociation constant (K_d) between JBC117 and the PHD was determined using SPR. Recombinant PHD was immobilized on the surface of the SPR sensor chip using the amine coupling method. We evaluated the binding of JBC117 to immobilized PHD using different concentrations of JBC117. The SPR data were fit with a 1:1 binding model of equilibrium analysis and the dissociation constant (K_d) was estimated to be 25 μM (Fig. 2d).

Inhibitory effect of JBC117 on β-catenin mediated transcription. To confirm the effect of JBC117 on the β-catenin-mediated transcriptional complex in cancer cells, we used the TOPFLASH/FOPFLASH reporter assay in HCT116, SW480 and A549 cell lines. The TOPFLASH construct contain two repeats of three optimal copies of the TCF/LEF binding sites, upstream of a thymidine kinase minimal promoter that is able to direct the transcription of the luciferase reporter gene. FOPFLASH contains mutated TCF/LEF binding sites, used as a negative control. LiCl (10 mM) was added to the cells to simulate the transcription of the Wnt luciferase reporter in cancer cell lines. Treatment with various concentrations of JBC117 inhibited β-catenin/TCF/LEF-mediated transcription in a dose-dependent manner, without significantly affecting FOPFLASH activity (Fig. 3a). We also used the q-PCR to examine the effect of JBC117 on the expression level of Wnt downstream target genes, including *Axin2*, *c-myc* and *cyclin D1*. JBC117

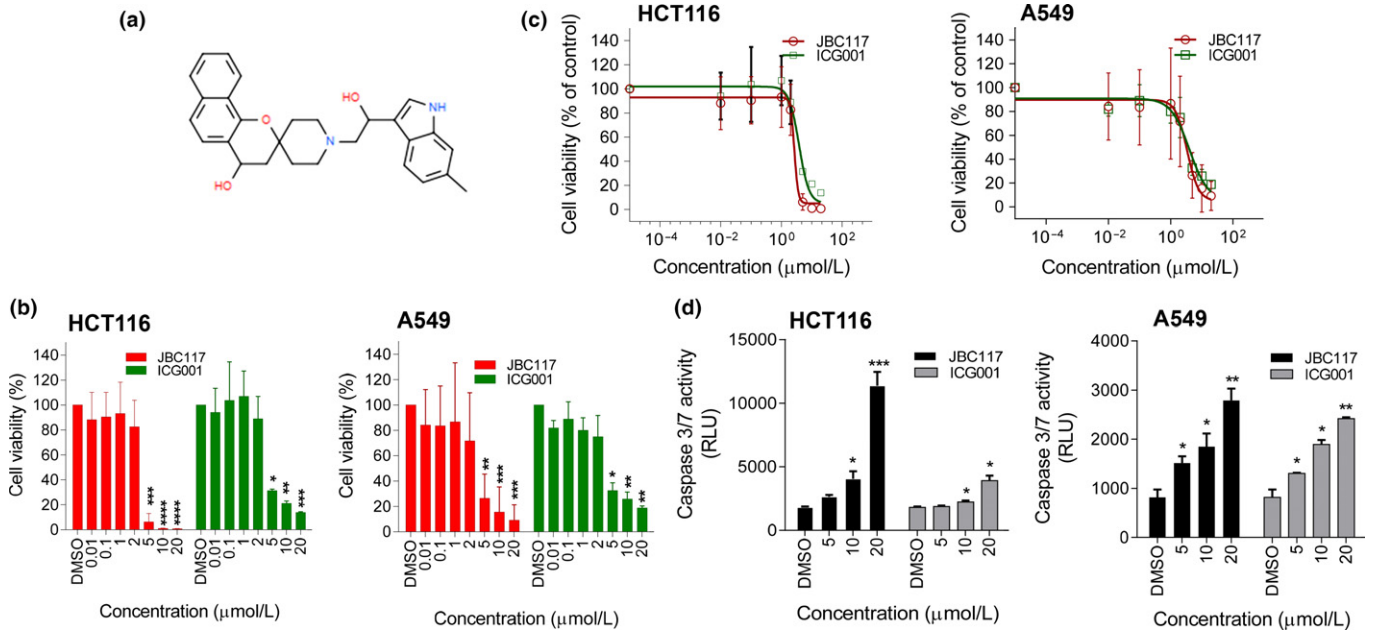

Fig. 1. JBC117 is selectively cytotoxic to the colon and lung cancer cells. (a) Chemical structure of JBC117. (b) Percentage cell viability of HCT116 and A549 cells, after exposure to increasing concentrations of JBC117 for 72 h. (c) IC_{50} values of JBC117 for HCT116 and A549 cells. (d) HCT116 and A549 were treated with JBC117 or ICG001 or DMSO. Caspase 3/7 enzymatic activity was measured. ICG001 was used as positive control. The data represent means ± SD of selected doses of three independent experiments. * indicates statistically significant values compared to DMSO (*P < 0.05, **P < 0.01 ***P < 0.001 and ****P < 0.0001).

Table 1. IC_{50} values of JBC117 and ICG001 on cancer cell line

IC_{50} (μmol/L)	JBC117	ICG001
HCT116	2.6 ± 0.16	3.8 ± 0.07
A549	3.3 ± 0.14	4.0 ± 0.08

significantly induced the downregulation of Wnt target genes in a dose-dependent manner (Fig. 3b). Western blot analysis also showed that treatment with JBC117 for 72 h suppressed the protein levels in a dose-dependent manner (Fig. 3c). Thus, these results indicated that JBC117 inhibited β-catenin mediated transcription.

Effects of JBC117 on the invasion, migration and tumorigenicity of colon and lung cancer. Cell motility and invasion are prerequisites for tumor progression and metastasis. Recently, it was reported that Pygo2 was associated with the invasion and angiogenesis of HCC tumor cells.[18] Therefore, we examined the effect of JBC117 or ICG001 on the invasive behavior of colon and lung cancer cells using Matrigel-coated Boyden chambers. The invasive ability of HCT116 and A549 cells was significantly lower in the presence of JBC117 than ICG001 (Fig. 4a,b). After 24 h of treatment with 20 μM JBC117, the invasion of HCT116 and A549 cells was approximately 8% and 2% of controls, respectively.

To further explore the effect of JBC117 on migration, we performed a wound-healing assay using HCT116 and A549 cell lines. JBC117 treatment significantly decreased the ability of HCT116 and A549 cells to migrate in a dose-dependent manner (Fig. 4c,d). These results suggest that JBC117 has an anti-invasive effect on colon and lung cancer cells.

We also examined the effect of JBC117 on anchorage-independent growth of HCT116 and A459 cancer cells. JBC117 efficiently inhibited the colony formation in soft agar in a dose-dependent manner (Fig. 5a). The IC_{50} values were 1.3 ± 0.87 μM (HCT116) and 1.5 ± 0.19 μM (A549) for JBC117, which were comparable to the values of 2.5 ± 0.15 μM (HCT116) and 1.7 ± 0.09 μM (A549) for ICG001. Next, we examined the effect of JBC117 on anchorage-dependent colony formation on 12-well plates. At 10 μM, JBC117 almost completely inhibited colony formation by HCT116 and A549 cells, which was similar to the effects of ICG001 (Fig. 5b).

Anti-tumor activity of JBC117 in mouse xenograft models of colon and lung cancer. We assessed the anti-tumor activity of JBC117 by using a xenograft of HCT116 and A549 cells established into the right flank of an individual athymic nude mouse. Once the tumor reached 225 mm^3 in size, mice were randomized into control and test groups and given a daily subcutaneous injection of either control solution, JBC117 (20 mg/kg/day), or ICG001 (20 mg/kg/day) for 14 successive days. Treatment with 20 mg/kg/day JBC117 significantly reduced colon and lung tumor growth by 65% and 93%, respectively, which was stronger than the inhibition by ICG001 (53% and 61% reduction of colon and lung tumor growth, respectively) (Fig. 6a,c). Quantitative analysis revealed that JBC117-mediated inhibition of xenograft tumor growth was statistically significant ($P < 0.05$) after 14 days of treatment (Fig. 6b,d). The survival of mice bearing the A549 tumor was analyzed by plotting Kaplan–Meier curves. The lifetime of mice treated with 10 mg/kg/day or 20 mg/kg/day JBC117 was significantly increased compared with control mice ($P < 0.0001$) (Fig. 6e). After terminating the administration of JBC117 at 85 days, all the treated mice were still alive even at 100 days (Fig. 6e). The body weight of xenograft mice was also monitored to examine the toxicity throughout the treatment period (Fig. 6f). JBC117

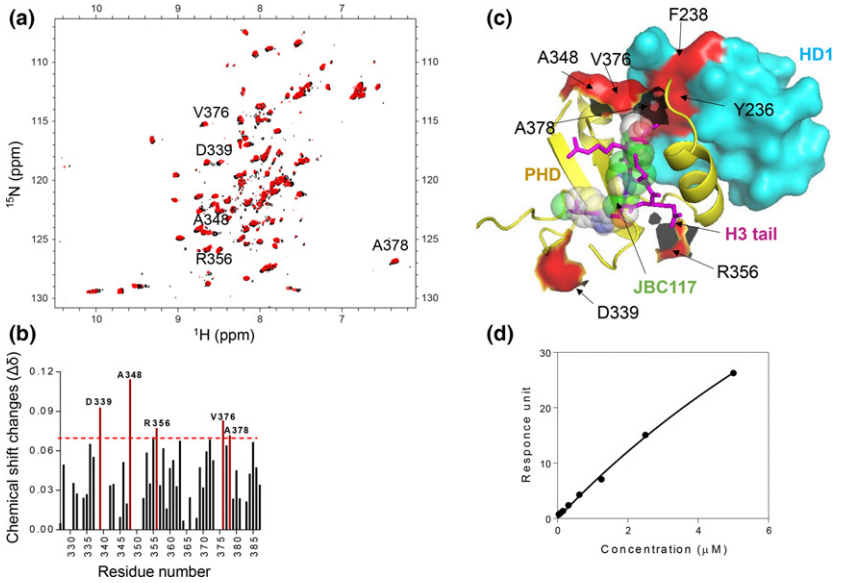

Fig. 2. Interaction of JBC117 with the recombinant PHD of Pygo2. (a) Overlay of the ^{1}H-^{15}N HSQC spectra of plant homeodomain (PHD) of pygo2 (327–387) in the absence (black) and presence (red) of JBC117. (b) Plot of chemical shift changes as a function of residue number comparing PHD alone and in the presence of 500 μM JBC117 (colored bar denotes the significant changes). The ^{1}H and ^{15}N chemical shift changes were calculated using the function $\Delta\delta = [(\Delta\delta\ ^{1}H)^{2} + 0.17(\Delta\delta\ ^{15}N)^{2}]^{1/2}$. The absence of a bar indicates proline residues, unmeasured shifts due to resonance overlaps or unassigned residues. The red colored line indicates the line for $\Delta\delta = 0.07$. The residues with $\Delta\delta > 0.07$ are indicated with a red bar. (c) Binding modes between JBC117 and PHD of Pygo2, obtained from NMR measurement (PDB entry: 2XB1). Surface (HD1) and ribbon (PHD) representation of the PHD-HD1 complex. Sticks indicate the histone 3 tail and spheres represent JBC117. Cyan, yellow and magenta colors represent the HD1, PHD and histone 3 tail, respectively. Red color indicates the residues with significant perturbations in chemical shift upon JBC117 binding. The model was generated using PyMOL. (d) Surface Plasmon Resonance shows the binding isotherm for the interaction between JBC117 and PHD under the assumption of a 1:1 binding model. K_d and Rmax values for JBC117 were estimated to be 25.3 μM and 157.7, respectively.

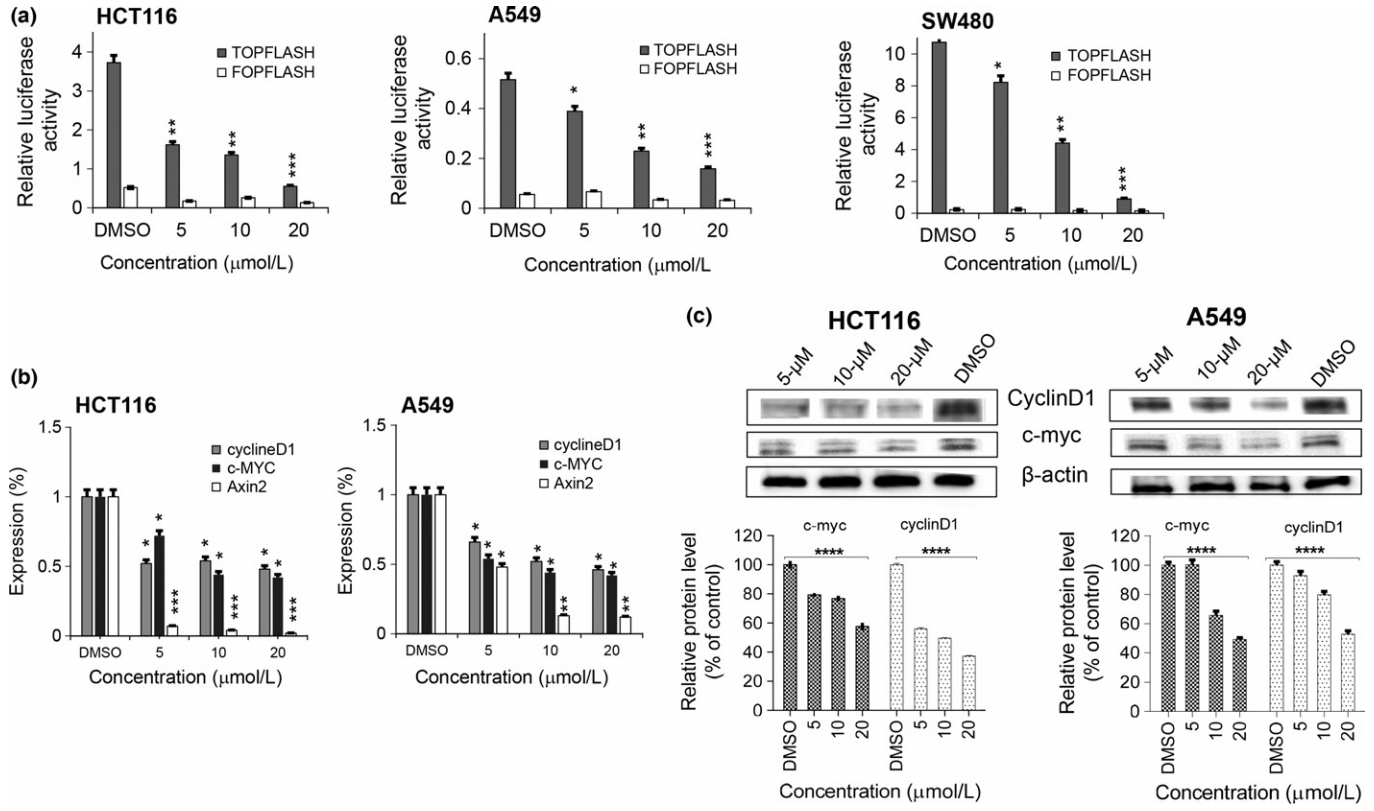

Fig. 3. Inhibitory effect of JBC117 on the transcriptional activity of β-catenin/TCF in colon and lung cancer cells. (a) JBC117 selectively inhibits the TCF reporter construct TOPFLASH but not FOPFLASH. (b) Quantitative real-time PCR showing the expression of Axin2, cyclinD1 and c-myc, normalized to GAPDH (housekeeping gene) in JBC117 treated HCT116 and A549 cells, respectively. The expression level of the control indicated as 1. (c) Western blot analysis showed that JBC117 inhibits the expression of target protein c-myc and cyclinD1 in HCT116 and A549 cancer cell lines. Quantification of the protein expression was performed using ImageJ software (NIH, Maryland, U.S). * indicates statistically significant values compared to DMSO (*$P < 0.05$, **$P < 0.01$ ***$P < 0.001$).

treatment did not induce a loss of body weight, whereas mice in the control group gradually lost body weight. The morphology of apoptotic cells was observed in tumor tissues by HE staining and cleaved caspase-3 immunostaining. HE staining revealed a decreased cellularity in the tumor mass in both HCT116 and A549 xenograft tumors following treatment with JBC117 compared with the control group (Fig. S5a). Furthermore, the cleaved caspase-3 immunostaining confirmed increased apoptosis in the tumor sections from the group treated with JBC117 relative to the control group (Fig. S5b). Caspase 3 plays a central role in chemotherapy-induced apoptosis.

Discussion

Aberrant activation of Wnt/β-catenin signaling is involved in the development and progression of many cancers.[5–9] In the Wnt transcription complex, targeting the β-catenin/TCF interface is crucial for drug design. However, targeting β-catenin is difficult because there are no enzymatic activators of β-catenin and the interaction between β-catenin and TCF is somewhat problematic as it shares between positive and negative regulators of the Wnt signaling pathway.[5,7] Interaction of β-catenin with essential transcription co-factors such as CBP, BCL9/BL9 and Pygo2 represents a promising target for blocking the β-catenin/TCF function in cancer cells.[2] It is reported that recruitment of these co-factors is essential for the β-catenin-TCF mediated transcriptions.[24,25] Disrupting the Pygo-BCL9/B9L-β-catenin interaction is promising because the function of Pygo-BCL9/B9L complex in Wnt signaling depends on three unique small protein–protein interactions. These interactions include interaction between PHD and its two ligands (HD1 and histone 3 tail) and interactions between BCL9/B9L and β-catenin.[12] Pygo2 also associates with histone-modifying enzymes such as histone methyltransferase and histone acetyltransferase. These molecular interactions allow Pygo2 to act as a chromatin effector that accelerates interpretation of the histone code.[26]

Nevertheless, there have been several evidence to develop the small molecule inhibitors that indirectly inhibit the oncogenic β-catenin by targeting one of its regulators. For example, ICG001,[24] IWR-1,[27] XAV939[28] and pyrvinium[29] indirectly inhibit β-catenin by interacting with CBP, porcupine, tankyrase and CK1α, respectively.

In this study, we identified a compound, JBC117, that selectively targets the PHD domain of Pygo2. JBC117 demonstrated a potent anti-cancer effect against colon and lung cancer both *ex vivo* and *in vivo*. We showed that low doses of JBC117 specifically inhibited the proliferation of human colon and lung cancer cells but was less toxic to non-cancerous human fibroblast cells. This feature implies the promising potential of JBC117 as an anticancer agent with a low risk of side effects. Moreover, JBC117 increases caspase activity in cancer cell lines. Caspases are cysteine endo-proteases that are activated in cells undergoing apoptosis. Our study also showed that JBC117 inhibited the TOPFLASH activity in both SW480 (APC mutants) and HCT116 (β-catenin mutants). JBC117 also inhibits the TOPFLASH activity in A549 cell lines. The inhibition of β-catenin-mediated transcription by JBC117 was also

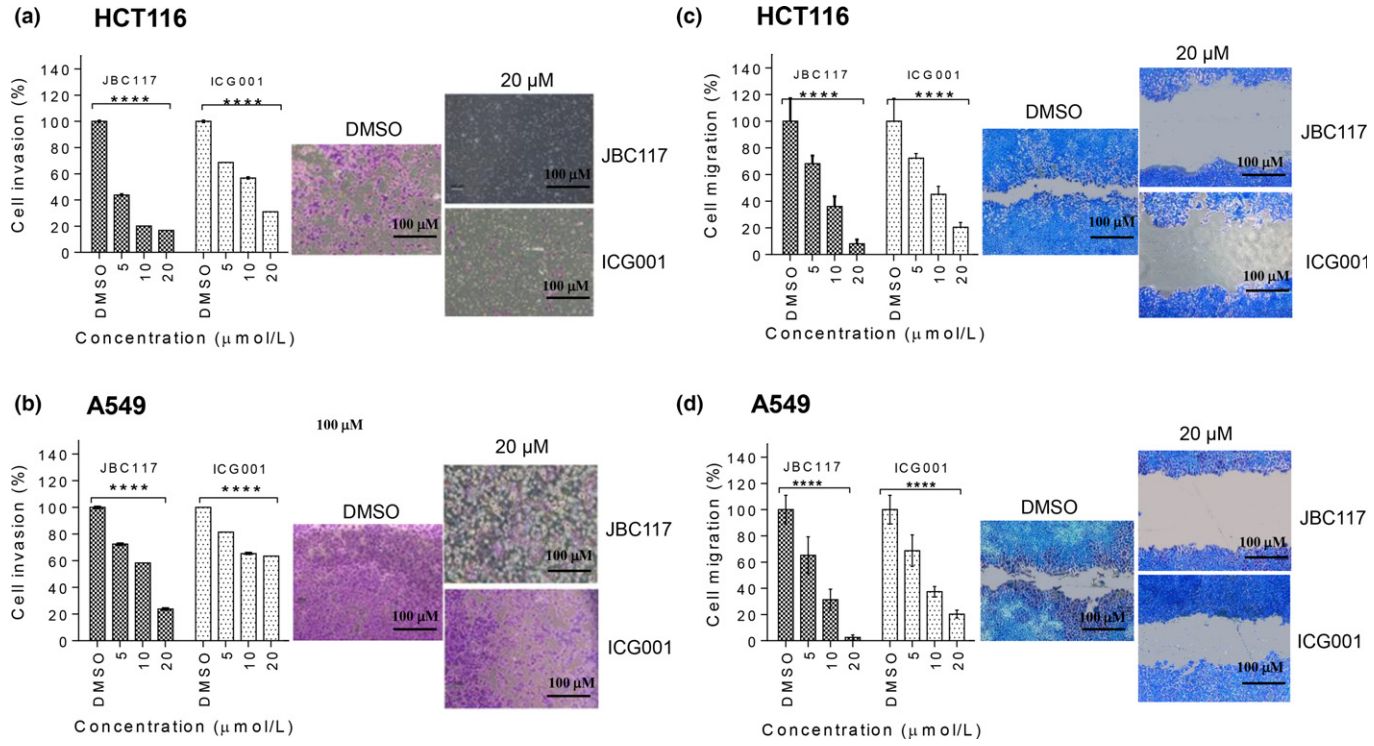

Fig. 4. JBC117 reduces the invasion and migration of HCT116 and A549 cells. (a) and (b) Transwell assay of invasive ability of HCT116 and A549 cells. Cells that invaded the bottom of the invasion membrane were stained and quantified at OD 560 nm after extraction. Data are mean ± SD of triplicate independent repeats. (c) and (d) Wound healing assay to measure cell migration in HCT116 and A549 cells; respectively. Cells were scratched with 200 μM pipet tip and treated with JBC117 for 24 h. The number of cells migrated into the wound was photographed and calculated as % of migration. ICG001 and DMSO were used as a positive and negative control, respectively. ****$P < 0.0001$, ANOVA.

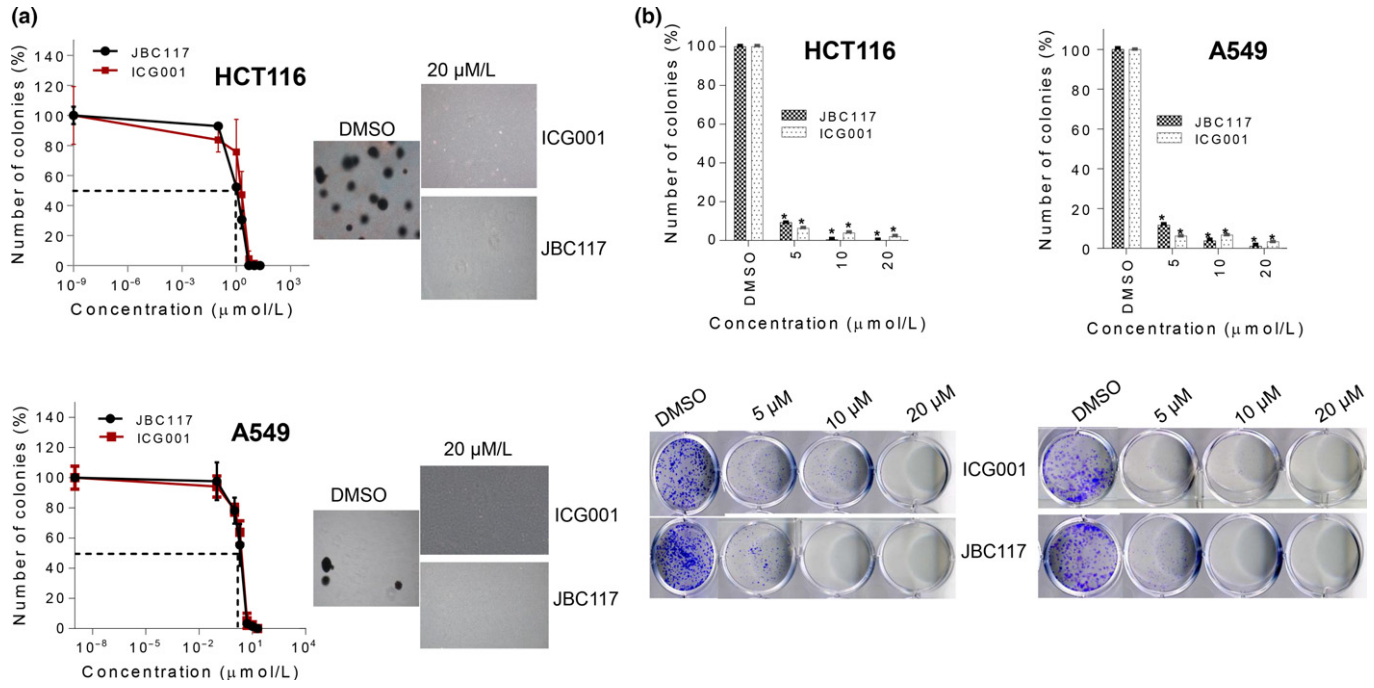

Fig. 5. JBC117 inhibits the formation of colonies by both cancer cell lines. (a) The soft agar assay using HCT116 and A459 cell lines. The cells were seeded into soft agar containing a various concentration of JBC117 or ICG001 and colonies were counted after 2 weeks. JBC117 efficiently inhibited the colony formation in a dose-dependent manner. (b) Colony formation assay of HCT116 and A549 cells treated with JBC117 at indicated concentrations. ICG001 was used as a positive control. *$P < 0.05$, ANOVA.

confirmed by the suppression of β-catenin-TCF target gene expressions, including *Axin2*, *c-myc* and *cyclinD1* in colon and lung cancer cell lines. The present data also showed that JBC117 markedly inhibited the invasive and migratory abilities of HCT116 and A549 cells. This may be attributed to inhibition of Pygo2, which plays an important role in controlling cell

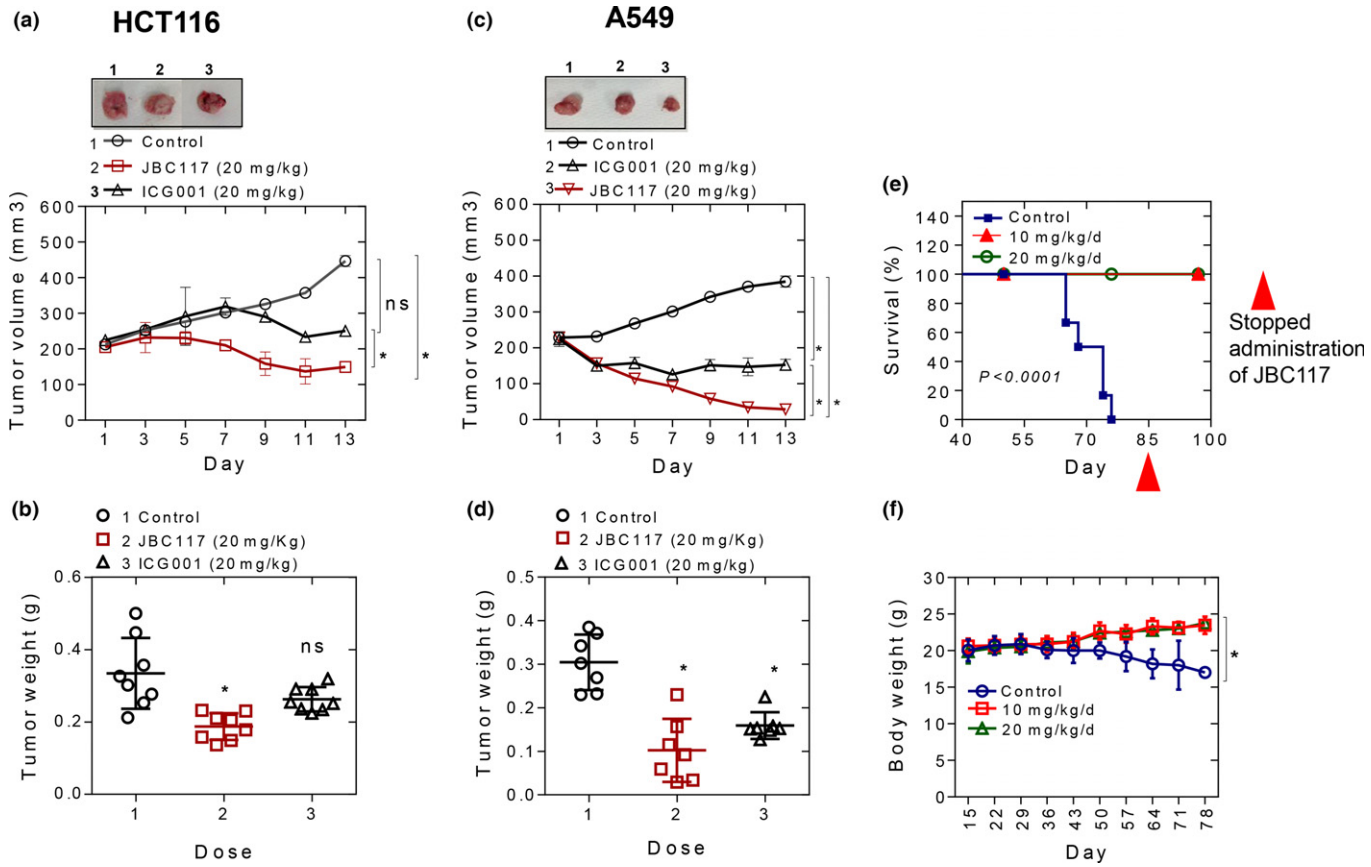

Fig. 6. Therapeutic efficacy of JBC117 in xenograft colon and lung cancer models. JBC117 significantly inhibited HCT116 (a and b) and A549 (c and d) tumor growth. (e) Effect of JBC117 on survival using the A549 xenograft tumor model. Mice were treated with JBC117 at the indicated doses (10 and 20 mg/kg/day). The survival of JBC117- treated and control mice were compared using the log-rank test and revealed significantly longer survival ($P < 0.0001$) in mice treated with JBC117 than control mice. We stopped the administration after 85 days. (f) Body weight of mice during treatment. *$P < 0.05$, student's *t*-test.

migration and cell invasion by regulating the expression of genes such as *MMP-2,-7*, *E-cadherin*. Recent evidence has also suggested that Pygo2 can increase cell migration and invasion by decreasing *E-cadherin* expression. By binding to the promoter region of *E-cadherin*, Pygo2 increases its methylation and also decreases zeb2 expression.[18] JBC117 also exhibited promising antitumor efficacy in HCT116 and A459 cells xenograft mice, which was consistent with its *ex vivo* anti-proliferative activity. JBC117-treated mice lived significantly longer than control mice and tumor tissues showed typical apoptotic characteristics.[30,31] This observed apoptosis may be attributed to the knockdown of Pygo2, which suppresses cell proliferation by blocking cell cycle progression from the G1 to S phase by downregulating cyclin D1.[19]

Binding studies using NMR revealed that JBC117 binds to D339 at the K4 pocket of the histone binding interface and A348 at the N-terminal alanine (A1) pocket of the PHD finger (Fig. 2c). The PHD finger binds to histone 3 tail through the two deep pockets: one is an anchoring pocket that covers its N-terminal alanine (A1) and the other is a specific pocket that embeds methylated lysine 4 (K4me).[6] The NMR data also showed that JBC117 interacts with V376, which formed a hydrogen bond with Y236 of HD1 and was involved in the main-chain interaction between PHD and HD1. JBC117 also binds to A378 of β-5 strand of PHD finger, which is directly linked to W377 that contributes to the structural PHD core.[6] Previous study also implied that V376 and A378 residues within β-5 strand of PHD interact simultaneously with Y236 and F238 of β-1 strand of HD1.[13] These interactions might indirectly influence the histone binding by affecting the affinity between PHD and HD1. Using fragment-based screening by NMR, Miller *et al.*[14] discovered a benzimidazole that docks into the histone 3 tail-specific pocket and displaces the native histone 3 tail of the PHD finger. It binds to the K4me pocket in PHD. They also discovered a set of benzothiazoles that bind to a cleft that emerges from the PHD–HD1 interfaces. Benzothiazoles form a hydrogen bond with D380 that constitutes the cleft gate. Several hydrophobic interactions occur between its benzene ring and F354 and A332 of PHD and between its thiazole and T359 of PHD. These interactions probably strengthen the interaction between benzothiazoles and the PHD–HD1 complex. However, these amino acids are not critical for the PHD–HD1 interface. We observed no cytotoxic effects of benzimidazole and a benzothiazole (2-Benzothiazolamine, 6-methoxy) in either colon or lung cancer cells (Fig. S4a,b). Unlike benzimidazole and benzothiazole, JBC117 simultaneously interferes with the native histone 3 tail and the PHD–HD1 interfaces. These findings suggest that the anticancer activity of JBC117 is dependent on specific disruption of the interaction between PHD and its two ligands, the histone 3 tail and HD1. We analyzed the binding of JBC117 to the recombinant PHD of Pygo2. We observed some non-specificity, which is sometimes inevitable, but JBC117, nonetheless, interacts strongly with Pygo2.

We also investigated the combined effect of JBC117 and ICG001 on colon and lung cancer cells. Interestingly, we found that JBC117 and ICG001 had a stronger anti-cancer effect when used in combination (Fig. S6a,b,c). Based on these findings, we propose that targeting Pygo2 and CBP, simultaneously, represents a more effective strategy for colon and lung cancer treatment.

In conclusion, using a strategy based on LDD, we identified a compound, JBC117, that binds to the PHD finger of Pygo2 and exhibits anti-proliferative activity toward cancer cells both *ex vivo* and *in vivo*. Therefore, selective targeting of the Pygo-BCL9 interface in cancer is highly promising for inhibiting the oncogenic Wnt pathway. Further studies would be needed to optimize the chemical structure of JBC117 and also to better understand the pharmacokinetics and pharmacodynamics to enable clinical application in the near future.

Acknowledgment

We thank Ms Sachie Hori for experimental assistance. We also thank Suez Canal University, Ismailia, Egypt for partially supporting Dr. Abdelazim. E. Elhelaly.

Disclosure Statement

The authors have no conflict of interest to declare.

References

1 Mosimann C, Hausmann G, Basler K. Beta-catenin hits chromatin: regulation of Wnt target gene activation. *Nat Rev Mol Cell Biol* 2009; **10**: 276–86.
2 Barker N, Clevers H. Mining the Wnt pathway for cancer therapeutics. *Nat Rev Drug Discov* 2006; **5**: 997–1014.
3 Clevers H, Nusse R. Wnt/beta-catenin signaling and disease. *Cell* 2012; **149**: 1192–205.
4 Polakis P. Drugging Wnt signalling in cancer. *EMBO J* 2012; **31**: 2737–46.
5 Polakis P. Wnt signaling in cancer. *Cold Spring Harb Perspect Biol* 2012; **4**: a008052.
6 Miller TC, Rutherford TJ, Johnson CM, Fiedler M, Bienz M. Allosteric remodelling of the histone H3 binding pocket in the Pygo2 PHD finger triggered by its binding to the B9L/BCL9 co-factor. *J Mol Biol* 2010; **401**: 969–84.
7 Thompson B, Townsley F, Rosin-Arbesfeld R, Musisi H, Bienz M. A new nuclear component of the Wnt signalling pathway. *Nat Cell Biol* 2002; **4**: 367–73.
8 Belenkaya TY, Han C, Standley HJ *et al.* Pygopus encodes a nuclear protein essential for wingless/Wnt signaling. *Development* 2002; **129**: 4089–101.
9 Kramps T, Peter O, Brunner E *et al.* Wnt/wingless signaling requires BCL9/legless-mediated recruitment of pygopus to the nuclear beta-catenin-TCF complex. *Cell* 2002; **109**: 47–60.
10 Parker DS, Jemison J, Cadigan KM. Pygopus, a nuclear PHD-finger protein required for Wingless signaling in Drosophila. *Development* 2002; **129**: 2565–76.
11 Gu B, Sun P, Yuan Y *et al.* Pygo2 expands mammary progenitor cells by facilitating histone H3 K4 methylation. *J Cell Biol* 2009; **185**: 811–26.
12 Fiedler M, Sanchez-Barrena MJ, Nekrasov M *et al.* Decoding of methylated histone H3 tail by the Pygo-BCL9 Wnt signaling complex. *Mol Cell* 2008; **30**: 507–18.
13 Adachi S, Jigami T, Yasui T *et al.* Role of a BCL9-related beta-catenin-binding protein, B9L, in tumorigenesis induced by aberrant activation of Wnt signaling. *Cancer Res* 2004; **64**: 8496–501.
14 Miller TC, Rutherford TJ, Birchall K, Chugh J, Fiedler M, Bienz M. Competitive binding of a benzimidazole to the histone-binding pocket of the Pygo PHD finger. *ACS Chem Biol* 2014; **9**: 2864–74.
15 Popadiuk CM, Xiong J, Wells MG *et al.* Antisense suppression of pygopus2 results in growth arrest of epithelial ovarian cancer. *Clin Cancer Res* 2006; **12**: 2216–23.
16 Andrews PG, Lake BB, Popadiuk C, Kao KR. Requirement of Pygopus 2 in breast cancer. *Int J Oncol* 2007; **30**: 357–63.
17 Tzenov YR, Andrews PG, Voisey K *et al.* Human papilloma virus (HPV) E7-mediated attenuation of retinoblastoma (Rb) induces hPygopus2 expression via Elf-1 in cervical cancer. *Mol Cancer Res* 2013; **11**: 19–30.
18 Zhang S, Li J, Liu P *et al.* Pygopus-2 promotes invasion and metastasis of hepatic carcinoma cell by decreasing E-cadherin expression. *Oncotarget* 2015; **6**: 11074–86.
19 Liu Y, Dong QZ, Wang S *et al.* Abnormal expression of Pygopus 2 correlates with a malignant phenotype in human lung cancer. *BMC Cancer* 2013; **13**: 346.
20 Torre LA, Bray F, Siegel RL, Ferlay J, Lortet-Tieulent J, Jemal A. Global cancer statistics, 2012. *CA Cancer J Clin* 2015; **65**: 87–108.
21 Siegel R, Desantis C, Jemal A. Colorectal cancer statistics, 2014. *CA Cancer J Clin* 2014; **64**: 104–17.
22 Kuwata K, Nishida N, Matsumoto T *et al.* Hot spots in prion protein for pathogenic conversion. *Proc Natl Acad Sci USA* 2007; **104**: 11921–6.
23 Ma B, Yamaguchi K, Fukuoka M, Kuwata K. Logical design of anti-prion agents using NAGARA. *Biochem Biophys Res Commun* 2016; **469**: 930–5.
24 Emami KH, Nguyen C, Ma H *et al.* A small molecule inhibitor of beta-catenin/CREB-binding protein transcription [corrected]. *Proc Natl Acad Sci USA* 2004; **101**: 12682–7.
25 Takada K, Zhu D, Bird GH *et al.* Targeted disruption of the BCL9/beta-catenin complex inhibits oncogenic Wnt signaling. *Sci Transl Med* 2012; **4**: 148ra17.
26 Gu B, Watanabe K, Dai X. Pygo2 regulates histone gene expression and H3 K56 acetylation in human mammary epithelial cells. *Cell Cycle* 2012; **11**: 79–87.
27 Chen B, Dodge ME, Tang W *et al.* Small molecule-mediated disruption of Wnt-dependent signaling in tissue regeneration and cancer. *Nat Chem Biol* 2009; **5**: 100–7.
28 Huang SM, Mishina YM, Liu S *et al.* Tankyrase inhibition stabilizes axin and antagonizes Wnt signalling. *Nature* 2009; **461**: 614–20.
29 Thorne CA, Hanson AJ, Schneider J *et al.* Small-molecule inhibition of Wnt signaling through activation of casein kinase 1alpha. *Nat Chem Biol* 2010; **6**: 829–36.
30 Saraste A, Pulkki K. Morphologic and biochemical hallmarks of apoptosis. *Cardiovasc Res* 2000; **45**: 528–37.
31 Hacker G. *The Morphology of Apoptosis*. *Cell and tissue research*. 2000; **301**(1):5–17.

Supporting Information

Additional Supporting Information may be found online in the supporting information tab for this article:

Fig. S1. Schematic diagram of the Wnt signaling pathway.

Fig. S2. *Ex vivo* cell proliferation assay of HCT116 and A549 cell lines.

Fig. S3. Effect of JBC117 on time-dependent manner in HCT116 and A549 cells and toxicity assay using human fibroblast cells.

Fig. S4. Effect of benzothiazole (2-Benzothiazolamine, 6-methoxy) and benzimidazole on colon and lung cancer cell lines.

Fig. S5. Histological examination of tumor tissues from HCT116 and A549 tumor xenograft mice.

Fig. S6. Synergistic effect of JBC117 and ICG001 against colon and lung cancer cells in *ex vivo*.

Data S1. Supporting materials and methods.